Scientific paper

Failure Mechanism of Foamed Concrete Made with/without Additives and Lightweight Aggregate

Ameer A. Hilal[1*], Nicholas H. Thom[2] and Andrew R. Dawson[3]

Received 24 June 2016, accepted 26 August 2016 doi:10.3151/jact.14.511

Abstract

It has been reported that owing to a densification of the internal structure of concrete, adding mineral admixtures leads to a more brittle behaviour. Therefore, with the intention of modifying (increasing the strength of) foamed concrete to make it suitable for structural purposes by means of admixtures and lightweight aggregate addition, the effect of these additions on the failure mechanism under compressive and tensile loading using different techniques is evaluated and discussed in this paper. Eight different mixes, made using a pre-formed foam, were investigated with varying density (different foam volumes), nominally 1300, 1600 and 1900 kg/m^3, without/with admixtures (silica fume, fly ash and superplasticizer) and lightweight aggregate. The Digital Image Correlation (DIC) technique was adopted to measure the deformations and strains on the surface of a specimen under uniaxial compressive load. Meanwhile, a Video Gauge technique was used to measure the horizontal deformation of discs during a splitting tensile test. From elasticity, fracture and fractal points of view, it was found that, for the same density, brittleness increases with many of the additives while it reduces with inclusion of lightweight aggregate. However, for all mixes, the lower the density (higher added foam volume), the higher the ductility.

1. Introduction

Although the use of foamed concrete has generally been limited to non-structural purposes such as filling of voids and cavities, backfill, bottom layers and to reduce the amount of settlement of buildings by reducing weight, its structural features are also of considerable interest.

The improvement (reduction in porosity) at the interface between the cement paste and aggregates due to Pozzolanic additions can affect the failure mechanism in concrete leading to increase/decrease in strength (Giaccio *et al*. 2007). In their study on the fracture characteristics of high performance concrete, Bharatkumar *et al* (2005) noticed a reduction in the compressive strength and fracture energy when using 25% and 50% replacements of cement by fly ash and slag. This was owing to the presence of larger unhydrated particles in the interfacial transition zone (ITZ) of the material, which had been intended to act as a high performance concrete, compared to normal concrete. However, Giaccio *et al* (2007) stated that this is not necessarily the case when a highly effective mineral such as silica fume (usually no more than 10% of cement weight) is used. Compared to conventional foamed concrete mixes, inclusion of admixtures in combination (fly ash, silica fume and superplasticizer) has been found to improve both the cement-paste microstructure and air-void structure of foamed concrete (Hilal *et al*. 2015b) leading to improved strength (Hilal *et al*. 2015c).

Regan and Arasteh (1990) stated that a foamed cement matrix and lightweight aggregate (LWA) combination, producing a lightweight aggregate foamed concrete, appears to offer a real weight saving, significant thermal insulation and sufficient strength for structural application with the possibility of casting in-situ with conventional equipment. In addition, they noticed that the behaviour (flexural and shear resistance) of reinforced members made of LWA foamed concrete was qualitatively similar to that of normal reinforced concrete. Before that, Weigler and Karl (1980) had concluded from the results of an investigation on lightweight aggregate foamed concrete that such material is suitable for heat insulating walls with a load bearing function.

1.1 Aims

Previous studies of foamed concrete (Kearsley 1999; Kearsley and Wainwright 2001; Jones and McCarthy 2006; Nambiar and Ramamurthy 2007a; Nambiar and Ramamurthy 2007b; Just and Middendorf 2009; Nambiar and Ramamurthy 2009; Yu *et al*. 2011) have focused on the investigation of its properties and the mix and preparation factors influencing them. As a result, knowledge of damage in foamed concrete under mechanical loading is limited. Therefore, this paper aims to investigate, from the fracture, elasticity and fractal points of view, the failure mechanism of foamed

[1]Lecturer, Department of Civil Engineering, Faculty of Engineering, University of Anbar, Iraq. *Corresponding author, *E-mail:* ameer_amn@uoanbar.edu.iq and ameer_amn@yahoo.com
[2]Lecturer, Department of Civil Engineering, Faculty of Engineering, University of Nottingham, University Park Nottingham, UK.
[3]Associate Professor, Department of Civil Engineering, Faculty of Engineering, University of Nottingham, University Park, Nottingham, UK.

concrete mixes having the same air void contents, for a given density, but with different matrices produced by using different additives (in combination) and LWA. This will be achieved by:

- Investigating the fracture energy and ductility under compressive and tensile loads from the load-deflection behaviour by adopting Digital Image Correlation (DIC) and Video Gauge techniques.
- Examining the critical stresses (the beginning of instability i.e. the onset of unstable propagation of cracks) from the stress-strain behaviour under compression.
- Examining the surface macrocracks under tensile loading by means of fractal dimension and then correlating the fractal dimension values with those of fracture energy.

2. Materials, mix proportions and production

Essential information can be summarized as follows:

2.1 Materials

To produce conventional foamed concrete (FC), the following constituent materials were used in this study:

- Portland cement, CEM I-52,5 N (3.15 S.G.) conforming to BS EN 197-1(2011).
- Natural sand (2.65 S.G.) conforming to BS 882 (1992) with additional sieving to remove particles greater than 2.36 mm.
- Fresh, clean and drinkable water.
- Foam (45 kg/m^3) was produced by blending the foaming agent, EABASSOC (1.05 S.G.), water and compressed air in predetermined proportions (45 g water to 0.8 ml foaming agent) in a foam generator, STONEFOAM-4.

The relevant mixtures are termed FC3, FC6 and FC9 being nominally 1300, 1600 and 1900 kg/m^3 in density, respectively. Then, to produce modified foamed concrete mixes suitable for structural purposes (FCx3 / FCx6 / FCx9), the following additives (the 'x' being a letter representing the additive type) were used depending on the desired mixes:

- Silica fume: Elkem Microsilica (2.2 S.G., 92% SiO_2, mean particle size 0.15 μm and specific surface 20 m^2/g) [x= 's'].
- Fly Ash: CEMEX fly ash-class S (2.09 S.G.) conforming to BS EN 405-1 (2005) [x= 'f'].
- Superplasticizer: MIGHTY 21 EG made by Kao Chemical GmbH of density 1.1 g/cm^3, compatible with the EABASSOC foaming agent [x= 'p'].

In addition, lightweight aggregate (LYTAG LWA) conforming to BS EN 13055-1 (2002) with a saturated surface dry specific gravity of 1.64 in its coarse (4-10mm) size was used in two mixes [x= 'y'] to examine its effect on the failure mechanism of foamed concrete.

2.2 Mix proportions and production

To make foamed concrete mixes suitable for structural purposes (denser than 1300 kg/m^3 and having more than 17 MPa compressive strength, (Neville 2011)), a preliminary experimental program (Hilal *et al.* 2015c), in terms of compressive strength tests, was carried out on the least dense mix (FC3, 1300 kg/m^3). Compared to a conventional mix FC3 (6 MPa 28-day compressive strength), adding 10% silica fume (FCs3), 20% fine sand replacement with fly ash (FCf3) and 1.5% superplasticizer by weight of binder (FCp3) individually improved the 28-day compressive strength by about 10% (to 6.5 MPa), 60% (to 9.5 MPa) and 115% (to 13 MPa), respectively. The compressive strength of FC3 increased by 125% (to 13.5 MPa) with a combination of silica fume and superplasticizer (FCsp3). In addition to adding silica fume and superplasticizer, fly ash replacement was limited, by trials, to 20% by weight of fine sand giving a compressive strength of 19 MPa (i.e. more than 17 MPa) and thereby bringing the FCsfp3 mix into the range where it may be considered as suitable for structural purposes (Neville, 2011). This large increase of 215% was achieved by adding the admixtures (silica fume, fly ash and superplasticizer) in combination. To enable sensible comparisons, similar proportions of the admixtures used in FCsfp3 were adopted for the 1600 and 1900 kg/m^3 mixes.

In this study, eight differently proportioned mixes were designed as follows: conventional mixes (FC) and modified mixes (FCsfp, hereinafter abbreviated to FCa) in which silica fume, fly ash and superplasticizer are combined together in the above proportions, see **Table 1**. Each was prepared at three nominal wet densities 1300 (FC3 and FCa3), 1600 (FC6 and FCa6) and 1900 (FC9 and FCa9) kg/m^3. Then two further mixes at 1600 kg/m^3 with LWA (FCy6 and FCya6) were added, replacing 25% of the sand, to investigate the effect of LWA on the failure mechanism, see **Table 1**.

As described in previous publications (Hilal *et al.* 2015b, 2015c), mix proportioning began with the selection of the target density (1300-1900 kg/m^3), the cement content and the water to cement ratio and the mix was proportioned by the method of absolute volumes. For each mix the water/binder ratio required to produce a stable mix (fresh density to target density ratio close to unity) was determined by trials while the required foam volume was determined from the mix design. LWA has low weight with high volume, therefore to leave enough space for foam bubbles, only 25% of sand weight was replaced by LWA (FCy6). To examine its effect on the failure pattern of foamed concrete. In addition, all the selected additives, with similar proportions as used in FCa6, were also added to this mix to produce a modified mix (FCya6).

In terms of production, the mixing sequence was: dry materials (including dry additives, if any), water (with dissolved superplasticizer, if any) to produce the base mix (unfoamed); and then foam to produce the foamed concrete. After that, the foamed concrete mix was placed in cubic and cylindrical moulds in two approxi-

Table 1 Mix proportions of the all selected foamed concrete mixes.

	FC3	FCa3	FC6	FCa6	FC9	FCa9	FCy6	FCya6
Target density (kg/m^3)	1300	1300	1600	1600	1900	1900	1600	1600
Cement content (kg/m^3)	500	450	500	450	500	450	500	450
Silica Fume (kg/m^3)	-	50	-	50	-	50	-	50
W/b ratio*	0.475	0.3	0.5	0.325	0.525	0.35	0.5	0.325
Superplasticizer (kg/m^3)	-	7.5	-	7.5	-	7.5	-	7.5
Water content (kg/m^3)	237.5	150	250	162.5	262.5	175	250	162.5
Sand content (kg/m^3)	562	514	850	744	1137.5	974	637.5	511.5
Fly Ash (kg/m^3)	-	128.5	-	186	-	243.5	-	186
LWA (kg/m^3)	-	-	-	-	-	-	212.5	232.5
Foam (kg/m^3)	19.4	19.4	13.3	13.3	7.6	7.6	10.5	10.5
Foaming agent (kg/m^3)	0.35	0.35	0.24	0.24	0.13	0.13	0.19	0.19
Foam (m^3)	0.424	0.424	0.295	0.295	0.166	0.166	0.233	0.233

*w/b ratios required to achieve a density ratio of about unity for the selected mixes

Table 2 Actual density, dry density, porosity and compressive strength values of the investigated foamed concrete mixes.

	FC3	FCa3	FC6	FCa6	FC9	FCa9	FCy6	FCya6
γ_{actual} (kg/m^3)	1295 (13.2)	1307 (15.2)	1621 (11.0)	1610 (12.8)	1875 (14.6)	1887 (8.1)	1603 (7.2)	1605 (12.7)
γ_{dry} (kg/m^3)	1137 (24.7)	1147 (18.2)	1466 (20.3)	1475 (10.5)	1778 (19.7)	1797 (6.1)	1457 (4.4)	1468 (14.0)
Porosity, φ_{vac} (%)	51.6 (0.2)	49.1 (0.3)	40.7 (0.3)	38.6 (0.6)	28.7 (0.7)	27.7 (0.5)	39.2 (0.3)	38.4 (0.7)
F_{cu}, 28 days, (MPa)	6.0 (0.3)	19.1 (0.7)	15.1 (1.3)	33.3 (0.7)	23.3 (0.8)	47.2 (0.9)	19.6 (2.1)	36.1 (1.7)

( ) includes the standard deviation values.

mately equal layers. After lightly tapping the mould sides, the surface of the layer subsided approximately to level (ASTM C796 1997), then the specimen surfaces were accurately levelled and covered with thick nylon to prevent evaporation. All specimens were removed from moulds within 24 hours. They were then sealed-cured (wrapped in cling film) and stored at about 20˚C until testing, since sealed-curing reflects typical industry practice for foamed concrete (Jones and McCarthy 2005).

Table 2 illustrates the actual and dry densities (γ_{act} and γ_{dry}) of the investigated mixes as well as their corresponding porosities (φ_{vac}) and compressive strengths (F_{cu}) at an age of 28 days. Note that the porosity was determined by means of a vacuum saturation method (Kearsley and Wainwright 2001) carried out on three samples for each mix. In addition, the 28-day compressive strength test was carried out on three cubic samples (100 mm^3) for each mix.

3. Experimental details

3.1 Digital Image Correlation technique (DIC)

Compared to other methods, there are some important advantages to using Digital Image Correlation (DIC) in studying the fracture of cementitious materials. Firstly, it does not have technical limitations relating to multiple cracks. Secondly, measured values of displacements would not be disturbed by the development of a crack because there is no need to attach gauges to the specimen and therefore the measurements of displacements are not disturbed while failure progresses. Thirdly, due to the use of different subset images for each measurement, displacement by this technique can be measured on the specimen while it is fractured into multiple parts during a loading test. Finally, unlike some sensitive techniques, the DIC method is not affected by vibration problems which are often generated by hydraulic testing machines (Shah and Choi 1999).

- The DIC technique has been used in various ways by many researchers because it is simple, full-field and contactless. It is a technique for large deformation/strain measurement at thousands of points on a specimen surface. Lecompte *et al.* (2006) defined DIC as an optical-numerical full-field displacement measuring technique which is based on a comparison between pictures taken during specimen loading.
- The displacements can be computed between two selected images, a reference and a deformed image, captured at different loading stages by using a charge-coupled device (CCD) camera. The idea is to track a point by means of the intensity (grey level) in the images. By repeating this process on a large number of subset images, full-field deformation or displacement data (with an accuracy of up to 1/100 pixel) can be obtained (Choi and Shah 1997; Lawler *et al.* 2001; Wang *et al.* 2010).
- For DIC investigation under compressive loading, two 50×50×100mm^3 prisms, cut from a 100×100×100mm^3 cube, were used. Since a concrete surface is relatively homogenous, images on

Table 3 Results of fracture energy and ductility.

Mixes	FC3	FC6	FC9	FCa3	FCa6	FCa9	FCy6	FCya6
W_f (kN.mm)	3.44	3.71	5.13	5.01	5.57	6.21	6.66	7.93
G_f (N/mm)	0.687	0.742	1.025	1.000	1.113	1.241	1.331	1.587
Peak Stress (MPa)	5.89	10.08	18.67	8.84	19.28	28.44	14.13	21.60
Ductility	0.117	0.074	0.055	0.113	0.058	0.044	0.094	0.073

it cannot be reliably matched. Therefore to make the surface heterogeneous, all specimens were painted first with white spray and then a black paint sprayed directly on the white surface in the form of dots.

- During testing, the compressive load was applied using an INSTRON machine, having a load capacity of 250 kN, by maintaining a constant rate of vertical deformation 0.0025 mm/s. Two digital cameras (CCD) with a resolution of (1392×1040 pixels) were used to acquire digital images of the specimen surface during each test. These images were sent to an image-processing computer with the capability of image storage, display and graphics.

3.2 Video Gauge technique

Splitting tensile tests were conducted on discs (100Ø×25 mm) with a Stingray camera (1388(h)×1038(v) pixels) and image processing software (Imetrum-Video Gauge) to measure the horizontal deformation between two points located near the middle of the specimen. This technique was used to avoid damage to linear variable differential transformers (LVDTs) at specimen failure. The principle of this technique is similar to that of the DIC technique.

4. Results and discussion

4.1 Fracture energy and ductility

Because of its stable pre-peak crack growth and strain-softening post peak, concrete is typically classified as a quasi-brittle material. Fracture mechanics has become a popular tool to quantify the brittleness of concrete (Babu 2008). Brittleness is commonly understood to be the tendency for a material to fracture suddenly before significant irreversible (plastic) deformation has developed.

The brittleness characteristic is proportional to fracture energy G_f (a high fracture energy leads to a tougher concrete) and also has typically an inverse dependence on strength f_c (stronger concrete is usually more brittle). Therefore, a balance between G_f and f_c is required to produce a ductile concrete (Rosselló *et al.* 2006). In other words, depending on the toughness/strength ratio (G_f/f_c), a relative ductility of the mix can be determined (Chiaia *et al.* 1998). Design of reinforced concrete structures is based on the ultimate strength capacity which includes a portion of the post-peak behaviour, i.e. strain-softening, of concrete in uniaxial compression. In addition, characterising the post-peak behaviour is necessary in predicting the ductility and ultimate axial deformation of concrete (Jansen and Shah 1997).

In their study of the deformation of concrete subject to compression, Choi and Shah (1997) found that a full-field measuring system based on DIC, compared to linear variable differential transformers (LVDT), was successfully able to measure the surface deformation in compression. In the current study, the load-displacement diagram was used to examine the compression fracture energy. From the DIC data, **Fig. 1** shows the full load-displacement relationship of different foamed concrete mixes, the average of two prisms (50×50×100 mm) for each mix, under uniaxial compressive load. In this study, there was a wide variation in the post-peak displacement of different specimens; therefore to evaluate comparable fracture energies it was decided to calculate up to 33% of the maximum load in the post-peak portion. The fracture energy (N/mm) was obtained by computing the work done W_f (the area under the load-displacement curve, kN.mm) (Jansen and Shah 1997) and dividing it by the cross-sectional area of the specimen (mm^2).

Table 3 summarises the results of work done, W_f, and fracture energy, G_f, for the investigated foamed concrete mixes. The FCa9 mix shows the highest peak load, whereas FCya6 is characterised by the highest fracture energy. If the work done (W_f) represents a measure of toughness (this property describes the ability of a material containing a crack to resist further fracture) (Chiaia *et al.* 1998), FCya6 is the toughest mix. On the other hand, from the brittleness point of view, mixes without additives (FC) are more ductile compared to those with silica fume, fly ash and superplasticizer additives having a similar density. This may be for two reasons:

- Firstly, inclusion of these additives helps to improve the matrix strength due to the additional reduction in porosity of the cement paste and an improved interface between it and the sand particles. As stated in (Hilal *et al.* 2015b), this matrix microstructure improvement can also be deduced from the difference between the vacuum saturation po-

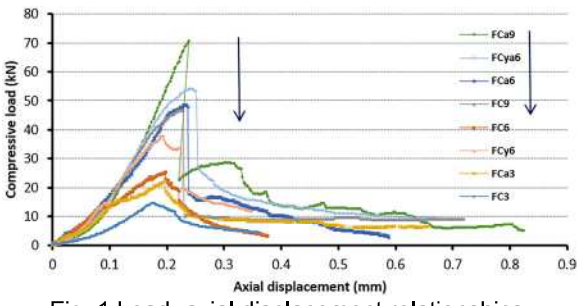

Fig. 1 Load- axial displacement relationships.

rosity, φ_{vac}, (entrained air voids and capillary voids) and the entrained (> 20μm) void content, φ_{OM}, calculated from analysis of optical microscopy images. It was found that the capillary porosity of FCa (with silica fume, fly ash and superplasticizer additives) is less than that of FC (without those additives). In addition, micro-hardness values of the ITZ at 30μm distance from the sand surface (five readings averaged from a Vickers micro-hardness test, square base pyramid indenter, with test load 10g and contact time 15s) were 39.66, 59.3 and 91.13 HV for FC3, FC6 and FC9 respectively while for FCa3, FCa6 and FCa9 they were 54.83, 85.56 and 111.43, respectively (where 1 HV=1 kgf/cm^3=0.09806650 MPa).

- Secondly, due to reduced size and connectivity of voids, by preventing their merging and producing a narrow void size distribution, inclusion of these additives achieved higher strength leading to brittle behaviour. In opposition to this, for all mixes, higher foam volume resulted in a greater degree of void merging, leading to large irregular voids which resulted in a wide distribution of void sizes and lower strength (Hilal *et al*. 2015a); as a result a more ductile behaviour was noticed, i. e. the lower the density the higher the ductility.

Compared to mixes without LWA, for a given density, inclusion of LWA leads to improved ductility with and without the other additives (i.e. FC6 and FCa6 mixes were more brittle than FCy6 and FCya6). This may be because of:

- Firstly, a good bond between the LWA and the surrounding hydrated cement paste as a consequence of several factors (Neville 2011) such as (i) good mechanical interlock due to the penetration of cement paste into the open surface pores in the LWA (ii) a small difference between the moduli of elasticity of the LWA and the cement paste; therefore, no differential stresses between these two materials are induced (iii) an additional hydration occurring in the LWA-cement paste interface zone due to the availability of water in the pre-wetted LWA or that absorbed by LWA during mixing. This strong bond leads to an absence of early development of ITZ (LWA-cement paste) microcracks, **Fig. 2** (**a, b** and **c**). Although microcracks will exist within the LWA particles, they will tend to be arrested by the improved ITZ, reducing the tendency to brittle failure.
- Secondly, the weakness of LWA causes a limited macro crack-arresting capacity and a stable manner of crack propagation through the LWA particles (Chiaia *et al*., 1998). In other words, most of the entrained voids (added pre-formed foam) are not connected at a macro level, **Fig. 2 (c)**, but the LWA particles represent very large voids with-connected porous texture making them the weakest regions. This causes the LWA particles to attract the main macrocracks (propagated from the voids and interfacial transition zone between cement paste and sand), **Fig. 2 (b, c** and **d)**, and increased ductility thereby results.
- Thirdly, replacing sand by LWA on the basis of mass results in, for a certain volume of concrete, proportionally less cement paste and more LWA

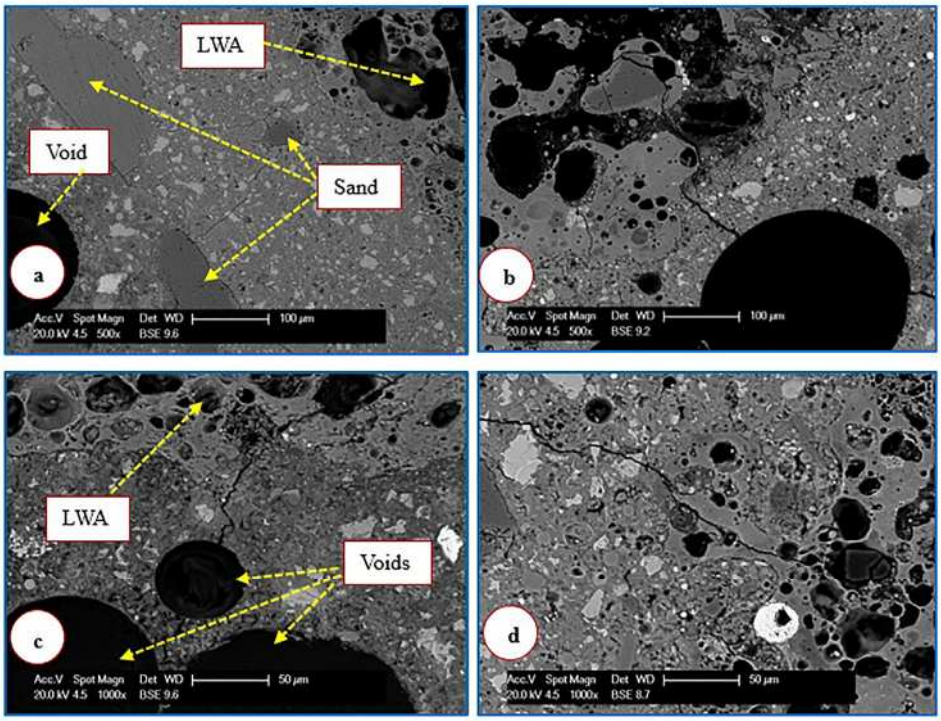

Fig. 2 SEM images showing microcracks propagation in mixes with LWA.

which may increase the likelihood of failure through the LWA particles.

The brittleness can also be deduced from the load-displacement curve; the steeper the slope of the descending branch, the more brittle is the material.

4.2 Load-deflection in tension

Two cylindrical specimens were tested (in splitting mode) for each mix and fitted lines showing averaged results are presented in **Fig. 3**. It can be seen that the curves for mixes with silica fume, fly ash and superplasticizer additives (FCa) are steeper than those for conventional mixes (FC) and this is also the case for mixes with LWA. If the lateral displacement represents the crack width, it is obvious that the crack width at failure increases with increased density, and for a given density it increases with the silica fume, fly ash and superplasticizer additives. In addition, using LWA helped to increase the crack width compared to a similar density mix without LWA. In general, for a given group (FC, FCa or FCy), the stronger the concrete the larger the lateral deformation before failure. During testing, it was noticed that, except for the FC3 mix, all investigated specimens split into two parts at the peak load, see **Fig. 4**. This prevented the complete load-deformation relationship from being obtained and thus there was no chance of calculating the fracture energy of the pre- and post-peak portions together in tension.

4.3 Stress-strain behaviour in compression

The failure of concrete under uniaxial compression is either a tensile failure of cement minerals (or of bond in a direction perpendicular to the applied load), or it is a collapse caused by the development of inclined shear planes (Neville 2011). Its mechanism involves the growth and propagation of cracks through the ITZ and mortar which are reflected in the stress-strain behaviour (Giaccio *et al.* 2007). Neville (2011) stated that one view of concrete failure is to associate it with the discontinuity point at which the volumetric strain ε_V stops decreasing due to development of extensive mortar cracks. This point represents the beginning of instability and sustained loading above this point will lead to failure.

It should be noted here that to measure the axial ε_A and lateral ε_L strains, vertical and horizontal potentiometers were fixed, as an initial trial, on a 150Ø×300 mm cylinder as shown in **Fig. 5 (a)**. However, it was found that the lateral strain behaviour (**Fig. 6**) was not compatible with that of brittle materials, such as concrete, even after changing the fixing method of the horizontal potentiometers, see **Fig. 5 (b)**. This led to a value for Poisons ratio (the ratio of the lateral strain to axial strain up to one-third of the ultimate stress) of about 0.4 for FCa3 and about 0.09 for FCa9. However, for concrete, the value normally lies in the range of 0.15 to 0.22 and it has been reported that it should be at the lower end of this range for lightweight concrete (Neville 2011). Therefore, it was decided to adopt Digital Image Correlation (DIC) since this has proved to be a successful system to measure deformation on a concrete surface (Choi and Shah 1997).

Based on the stress-strain curves obtained from the

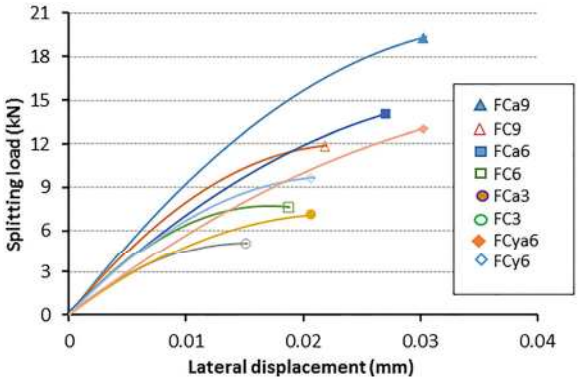

Fig. 3 Splitting load versus lateral displacement of the investigated mixes.

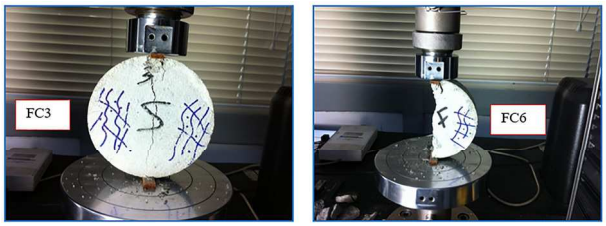

Fig. 4 Specimen failure after splitting test.

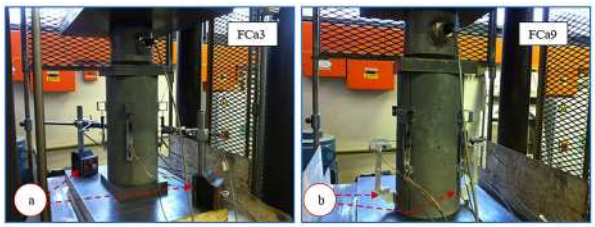

Fig. 5 (a) Horizontal potentiometers fixed on the base (b) Horizontal potentiometers fixed on the specimen.

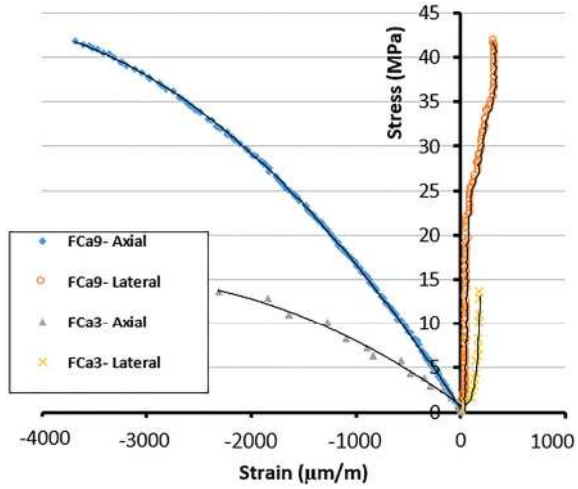

Fig. 6 Stress versus axial and lateral strains in compression using horizontal and vertical potentiometers.

DIC data, **Fig. 7**, the critical stresses can be obtained. The critical stresses represent the onset of unstable propagation of cracks in the concrete matrix and are defined as the stresses corresponding to the minimum peak in the volumetric strain curves ($\varepsilon_V=\varepsilon_A+2\varepsilon_L$) (Giaccio *et al*. 2007). The results of critical stresses as percentages of the corresponding compressive strengths are shown in **Fig. 8**. As can be observed from this figure, the percentage increases with increased density (reduced added foam) and for a given density it increases with inclusion of the silica fume, fly ash and superplasticizer additives. This indicates that the period of unstable crack propagation through the mortar matrix (between the critical and peak stresses) is reduced, showing a tendency to a more brittle failure mechanism. In addition, adding LWA helped in decreasing the critical stress percentage leading to more ductile behaviour compared to mixes with the same density but without LWA.

4.4 Fractal dimension

Macrocracks on the surfaces of disc specimens (100Ø×25 mm, tested in splitting tensile mode) were examined by means of fractal dimension (D). D is a measure of how complex a failure surface is, quantifying the pattern failure complexity, statically, as a ratio of the change in details to the scale at which they are measured. The fractal dimensions of cracks were computed by means of the box-counting method in ImageJ software. In this method, the digitized crack is covered with a rectangular mesh with different grid sizes (x_1, x_2, …). By varying x and counting the number of grids, a logarithmic plot of log(N) versus log(1/x) can be drawn. The slope of the fitting line is the fractal dimension D.

It can be seen from **Fig. 9** that with incorporation of the silica fume, fly ash and superplasticizer additives, the surface macrocrack of FCa9 becomes more complicated making its fractal dimension higher than that of the conventional mix (FC9). Since the density increases with reducing added foam, i.e. larger distances between voids, the fractal dimension of FC9/FCa9 is higher than that of FC3/FCa3 indicating that the failure (normally through the voids) of the former is more complicated than that of the latter, see **Fig. 10**. **Figure 10** also shows the fractal dimensions plotted against the fracture energies of the selected mixes. It can be seen that D decreases with increased added foam and with a given density it increases with all additives. It should be mentioned here that the main crack propagates preferentially through the LWA particles which represent the weakest regions because of their connected cellular texture, see **Fig. 11**, resulting in a "zigzag" failure crack (higher D) compared to mixes with the same density but without LWA. However, this "high D" does not mean that the FCy6/ FCya6 mix is more brittle than the FC6/FCa6 mix. It should be noted here that for each mix, from an image analysis using the ImageJ software on fractured surface images (**Fig. 11**), the percentage of LWA (by volume) on the fractured surfaces (24% for FCy6 and

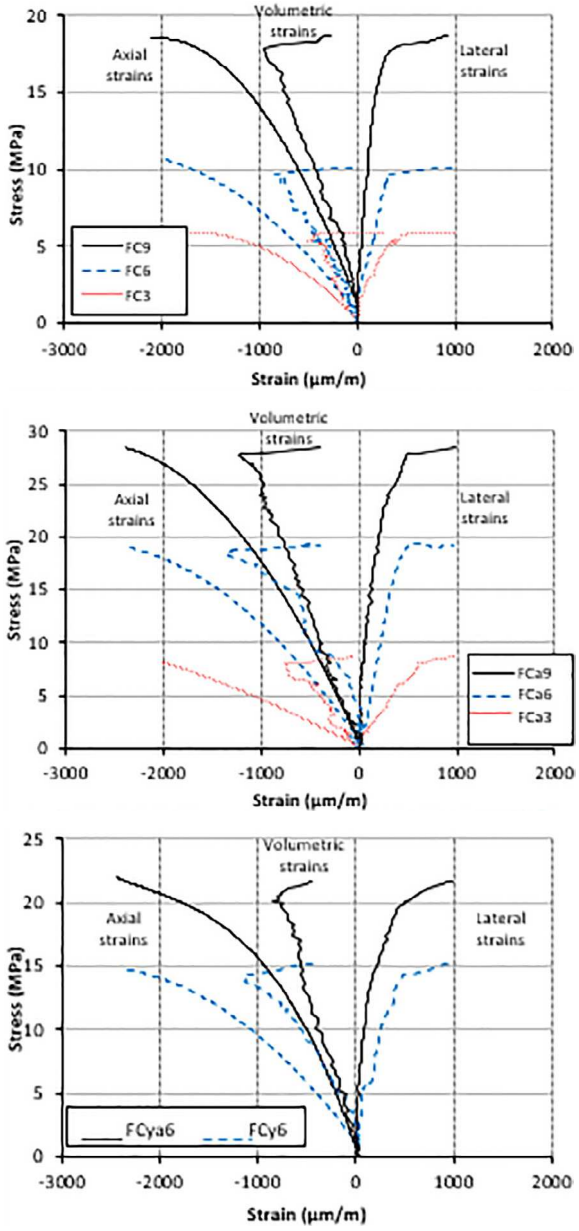

Fig. 7 Stress versus axial, lateral and volumetric strains in compression using DIC technique.

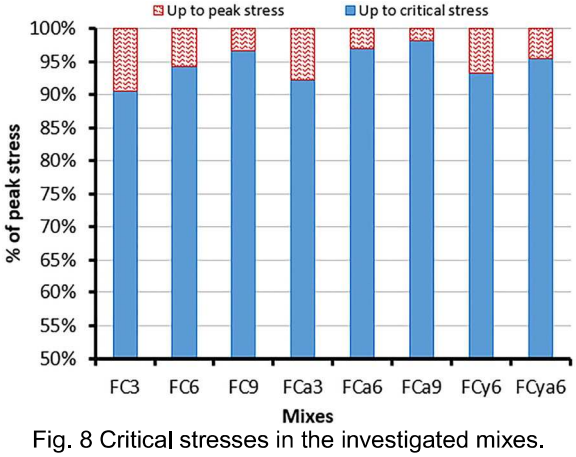

Fig. 8 Critical stresses in the investigated mixes.

21% for FCya6) was higher than that in the mix (13% for FCy6 and 14% for FCya6), proving that the main crack goes through the LWA particles in a zigzag way. The splitting failure pattern of some of the specimens is shown in **Fig. 12**.

Charkaluk *et al*. (1998) stated that a general conclusion cannot easily be drawn about the correlation of fractal dimension of fractured surfaces with fracture toughness since some workers have reported a positive variation while others have found it to be negative. However, from **Fig. 10**, it is evident that there is a good correlation between the fractal dimensions and the fracture energies of the foamed concrete mixes investigated in this research.

5. Conclusions

In this study, eight different foamed concrete mixes, made using a pre-formed foam, with varying density (different foam volumes), nominally 1300, 1600 and 1900 kg/m^3, without/with admixtures (silica fume, fly ash and superplasticizer) and lightweight aggregate were investigated. Their failure mechanism under compressive and tensile loading using different techniques is evaluated and discussed in this paper. Based on the results and discussion, the following conclusions are made:

(1) From a brittleness point of view:

- Mixes without silica fume, fly ash and superplasticizer (FC) are more ductile compared to those with these additives having a similar density.
- Compared to mixes without LWA, for a given density, inclusion of LWA leads to improved ductility of mix with and without the other additives.

(2) From a fracture point of view:

- During a splitting tensile test, the stronger the concrete (increased density or silica fume, fly ash and superplasticizer additives used) the larger the lateral deformation (crack width) before failure.
- The percentage of critical stress increases with increased density (reduced added foam) and for a given density it increases with inclusion of silica fume, fly ash and superplasticizer additives in combination showing a tendency to a more brittle

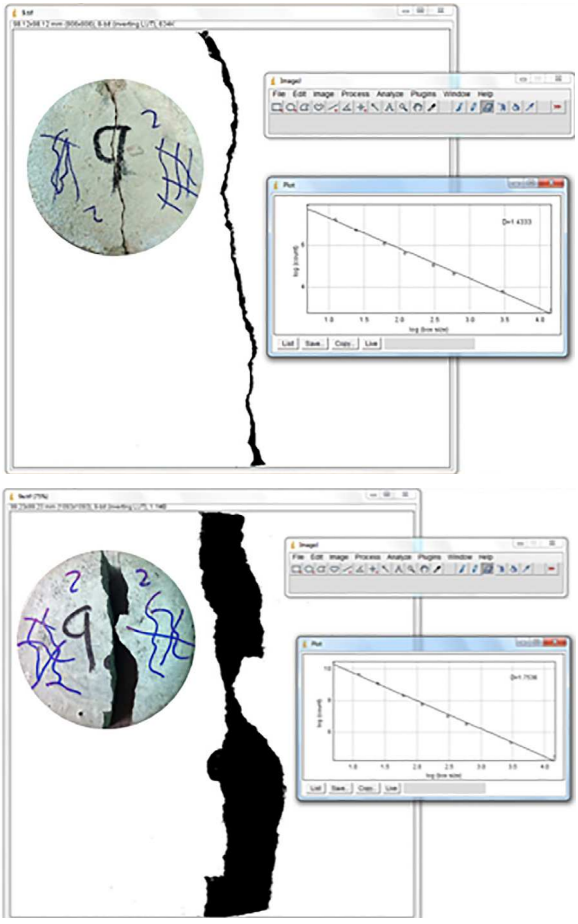

Fig. 9 Fractal dimension of FC9 (above) and FCa9 (below) mixes.

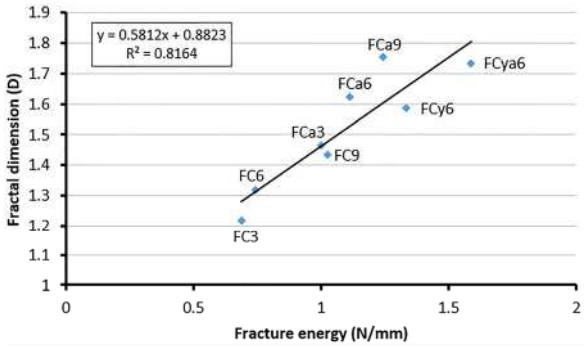

Fig. 10 Relationship between the fractal dimension and the fracture energy.

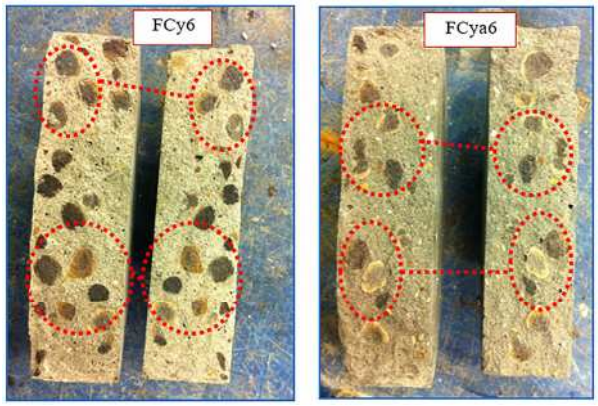

Fig. 11 Macrocrack through LWA particles during splitting test.

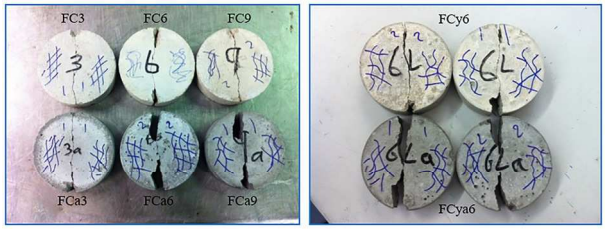

Fig. 12 Failure pattern of selected specimens.

failure mechanism.

- Adding LWA helped in decreasing the percentage of critical stress leading to more ductile behaviour compared to mixes with the same density but without LWA.

(3) From a fractal point of view:

- The fractal dimension deceases with increase in the amount of added foam and for a given density it increases with all types of additives.
- It was found that there is a good correlation between the fractal dimension and the fracture energy for the foamed concrete mixes investigated in this study.

(4) In general, from the elasticity, fracture and fractal points of view, it was found that, for the same density, brittleness increases with silica fume, fly ash and superplasticizer additives (due to improved matrix and reduced void sizes and connectivity) while it reduces with inclusion of LWA (due to microcracks being arrested at the early stages of loading and due to LWA's ability to attract the main macrocracks at the failure stage). However, for all mixes, (due to a greater degree of void merging) the lower the density (higher added foam volume) the higher the ductility.

This study has suggested a number of avenues for future research including:

(1) Modifying brittleness behaviour to gain greater post-peak load capacity (for safety considerations); one way this might be possible could be by adding fibres.

(2) Investigating the initiation and propagation of micro and macrocracks in foamed concrete mixes under mechanical loading by adopting internal and surface investigation techniques.

Acknowledgements

The authors would like to acknowledge the support of the Higher Committee for Education Development in Iraq (HCED) for the research scholarship enabling this work to be conducted as part of a larger research project. The valuable help and comments of Mr Thomas Buss (University of Nottingham) during the DIC and video gauge observations are gratefully acknowledged.

References

ASTM C796, (1997). "*Standard test method for foaming agent for use in producing cellular concrete using preformed foam.*" American Society for Testing and Materials.

Babu, D. S., (2008). "*Mechanical and deformational properties, and shrinkage cracking behaviour of lightweight concretes.*" Thesis (PhD). National University of Singapore.

Bharatkumar, B. H., Raghuprasad, B. K., Ramachandramurthy, D. S., Narayanan, R. and Gopalakrishnan, S., (2005). "Effect of fly ash and slag on the fracture characteristics of high performance concrete." *Materials and Structures*, 38, 63-72.

BS 882, (1992). "*Specification for aggregates from natural sources for concrete.*" British Standards Institution, London.

BS EN 197-1 (2011). "*Cement-Part 1: Composition, specifications and conformity criteria for common cements.*" British Standards Institution, London.

BS EN 405-1, (2005). "*Fly ash for concrete- Part 1: Defination, specifications and conformity criteria.*" British Standards Institution, London.

BS EN 13055-1, (2002). "Lightweight aggregates- part 1: Lightweight aggregates for concrete, mortar and grout." British Standards Institution, London.

Charkaluk, E., Bigerelle, M. and Iost, A., (1998). "Fractals and fracture." *Engineering Fracture Mechanics*, 61, 119-139.

Chiaia, B., van Mier, J. G. M. and Vervuurt, A., (1998). "Crack growth mechanisms in four different concretes: microscopic observations and fractal analysis." *Cement and concrete research*, 28, 103-114.

Choi, S. and Shah, S., (1997). "Measurement of deformations on concrete subjected to compression using image correlation." *Experimental Mechanics*, 37, 307-313.

Giaccio, G., de Sensale, G. R. and Zerbino, R., (2007). "Failure mechanism of normal and high-strength concrete with rice-husk ash." *Cement and Concrete Composites*, 29, 566-574.

Hilal, A. A., Thom, N. H. and Dawson, A. R., (2015a). "On entrained pore size distribution of foamed concrete." *Construction and Building Materials*, 75, 227-233.

Hilal, A. A., Thom, N. H. and Dawson, A. R., (2015b). "On void structure and strength of foamed concrete made without/with additives." *Construction and Building Materials*, 85, 157-164.

Hilal, A. A., Thom, N. H. and Dawson, A. R., (2015c). "The use of additives to enhance properties of preformed foamed concrete." *International Journal of Engineering and Technology*, 7, 286-293.

Jansen, D. C. and Shah, S. P., (1997). "Effect of length on compressive strain softening of concrete." *Journal of engineering mechanics*, 123, 25-35.

Jones, M. and McCarthy, A., (2005). "Preliminary views on the potential of foamed concrete as a structural material." *Magazine of concrete research*, 57, 21-31.

Jones, M. R. and McCarthy, A., (2006). "Heat of hydration in foamed concrete: Effect of mix constituents and plastic density." *Cement and concrete research*, 36, 1032-1041.

Just, A. and Middendorf, B., (2009). "Microstructure of high-strength foam concrete." *Materials Characterization*, 60, 741-748.

Kearsley, E., (1999). "*The effect of high volume of ungraded fly ash on the properties of foamed concrete.*" Thesis (PhD). The University of Leeds.

Kearsley, E. and Wainwright, P., (2001). "Porosity and permeability of foamed concrete." *Cement and concrete research*, 31, 805-812.

Lawler, J. S., Keane, D. T. and Shah, S. P., (2001).

"Measuring three-dimensional damage in concrete under compression." *ACI Materials Journal*, 98, 465-475

Lecompte, D., Smits, A., Bossuyt, S., Sol, H., Vantomme, J., Van Hemelrijck, D. and Habraken, A. M., (2006). "Quality assessment of speckle patterns for digital image correlation." *Optics and Lasers in Engineering*, 44, 1132-1145.

Nambiar, E. and Ramamurthy, K., (2007a). "Air-void characterisation of foam concrete." *Cement and concrete research*, 37, 221-230.

Nambiar, E. K. K. and Ramamurthy, K., (2007b). "Sorption characteristics of foam concrete." *Cement and concrete research*, 37, 1341-1347.

Nambiar, E. K. K. and Ramamurthy, K., (2009). "Shrinkage behavior of foam concrete." *Journal of materials in civil engineering*, 21, 631.

Neville, A. M., (2011). "*Properties of concrete*." *5th.* London Pearson Education Limited.

Regan, P. and Arasteh, A., (1990). "Lightweight aggregate foamed concrete." *Structural Engineer,* 68, 167-173.

Rosselló, C., Elices, M. and Guinea, G. V., (2006). "Fracture of model concrete: 2. Fracture energy and characteristic length." *Cement and concrete research,* 36, 1345-1353.

Shah, S. and Choi, S., (1999). "Nondestructive techniques for studying fracture processes in concrete." *International journal of fracture*, 98, 351-359.

Wang, Y. H., Jiang, J. H., Wanintrudal, C., Du, C., Zhou, D., Smith, L. M. and Yang, L. X., (2010). "Whole field sheet-metal tensile test using digital image correlation." *Experimental Techniques*, 34, 54-59.

Weigler, H. and Karl, S., (1980). "Structural lightweight aggregate concrete with reduced density--lightweight aggregate foamed concrete." *International Journal of Cement Composites and Lightweight Concrete*, 2, 101-104.

Yu, X. G., Luo, S. S., Gao, Y. N., Wang, H. F., Li, Y. X., Wei, Y. R. and Wang, X. J., (2011). "Pore structure and microstructure of foam concrete." *Advanced Materials Research*, 177, 530-532.